Chapter 4

INTRODUCTION

The goal of this research is to determine if cooperativity can be used to provide a link between the molecular structure of an interphase and the final mechanical properties of a composite material. An interphase may be defined in composites as a three dimensional region that immediately surrounds the fiber and has attributes that differ from the bulk matrix material. This micro-scale region that often makes up less than 1 weight percent of the composite has been shown experimentally by several authors to have a dramatic influence on performance[4.1-4.4]. The properties that are influenced range from tension, compression, toughness, fatigue and hygrothermal resistance. A comprehensive understanding of the composite interphase role in behavior is still lacking however. This is in part due to the several complexities involved. For example, polymer-polymer interdiffusion leads to a difficult graded material characterization problem. And, a strong multidisciplinary approach to relate mechanical properties to molecular understanding is needed.

There are many articles in the literature that describes the character of the interfacial properties of composite materials using data from dynamic mechanical analysis (DMA). Lewis and Nielsen[4.5] performed an early comprehensive study of an A-glass bead filled epoxy composite that is frequently cited. These researchers were primarily interested in determining the relative shear modulus of the filled epoxy composite in comparison to an unfilled epoxy control sample. It was observed that the relative shear modulus increased with increasing volume fraction of filler and decreasing particle size. The effect of increasing shear modulus was more pronounced in the rubbery response region at temperatures above the glass transition temperature (T_g). A slight temperature dependence of the relative shear modulus was also observed in the glassy region, but this was attributed to residual stresses due to a mismatch between the coefficients of thermal expansion for the glass filler and epoxy matrix.

In their study, Lewis and Nielsen also examined the viscoelastic effects of pretreating the glass filler with different coupling agents. Methylchlorosilane (MCS) and γ-glycidoxypropyltriethoxysilane (GPS) were used to promote poor or good adhesion,

respectively, between the filler and matrix epoxy. No noticeable effects of varying coupling agents were observed in the shear storage modulus curves. However, the shear loss modulus and damping (tan δ) curves varied significantly depending on the coupling agent that was used. The damping in the MCS case was greater than was found for the GPS pretreated composite. The width of the tan δ curve was also wider for the GPS treated composite. Lewis and Neilsen believed that these changes in amplitude and width of the damping curves were caused by the specific interfacial interactions between the epoxy matrix and glass filler.

Cousin and Smith[4.6] observed changes in the tan δ curves of a sulfonated polystyrene ionomer that had been filled with small diameter alumina particles. The addition of the filler resulted in a broadening of the tan δ peak, as well as a decrease in the peak maximum amplitude, at the glass transition. They attributed the changes in the tan δ curves to the degree of the polymer-filler interactions occurring at this interface. Cousin and Smith also state that strong polymer-filler interactions will decrease the mobility and free volume of the polymer chains near the particle surface.

Eisenberg and Tsagaropoulos[4.7, 4.8] theorized that two distinct regions of restricted mobility exist near the filler-polymer interface. The polymer chains nearest to the filler particle are tightly bound and are so highly restricted in mobility that they cannot participate in any transitions that are measurable by DMA. Beyond these tightly bound chains are loosely bound chains. There, they postulated chains that are more restricted in mobility when compared to the bulk polymer phase, but not as restricted as the tightly bound chains. If this model is correct then the differences in the damping curves of composite materials can be attributed to viscoelastic changes in the interphase region surrounding the filler particle. For example, a broadening in tan δ is predicted.

Reed[4.9] performed dynamic mechanical tests on glass fiber reinforced epoxy matrix composites and observed a new thermal transition above the glass transition. Reed hypothesized that the existence of a resin region entrapped near the interface with a differing network structure was the cause for this higher temperature thermal transition. This additional transition also was detected as a change in thermal expansion coefficient in thermal experiments.

Thomason[4.10] performed dynamic mechanical tests on several different composites comprised of glass fiber reinforced epoxy. Several different glass fibers from different vendors were tested along with one carbon fiber composite. The appearance of the second transition at a temperature higher than the glass transition temperature was reported to exist only in the case of the glass fiber composites. Thomason attributed the second peak to be an artifact caused thermal lag during heating of the sample, which results primarily from the low thermal conduction of the glass fibers. An artificial second peak can then originate because of a fast sample-heating rate, poor thermal conductivity of the composite, and residual stresses in the composite. The glass transition for the clamped portion of the composite sample simply falls behind glass-to-rubber transition of the suspended portion between the DMA clamps, giving a second transition peak at a higher temperature. This argument was supported by the disappearance of the transition in the case of the carbon fiber specimens where there is a greater thermal conductivity. Thomason recommended using heating rates below 5°C/min to prevent this problem.

A broadening of the loss modulus and tan δ curves in composite materials when compared to neat resins can be credited to an increase in the breadth of the distribution of relaxation times (τ). Landel[4.11] observed these phenomena while studying the relaxation spectra of polyisobutylene that had been filled with glass beads. Fitzgerald, *et al.*[4.12] considered the effects of the addition of a silicate network to the distribution of relaxation times in polyvinylacetate (PVAc). Fitzgerald , *et al.* created dielectric loss master curves in the frequency domain for the PVAc/silicate composites. These master curves were then fitted to the Kohlrausch-Williams-Watts equation (1) to quantify the width of the distribution of relaxation times.

$$\phi(t) = \exp[-(t/\tau)^{(1-n)}] \qquad (1)$$

In this equation (1) ϕ(t) is the Kohlrausch transient response function and *n* is the coupling constant.[4.13] The coupling constant parameter provides a measure of the width of the distribution of relaxation times.[4.14] When *n* is equal to 0 then the KWW equation describes the single relaxation time of a simple exponential decay.[4.15] In frequency space a simple Debye oscillator is imagined. However, the molecular environment of a polymer is much more complicated than the Debye model of simple rigid spheres, which are surrounded by a viscous fluid. Because of this complicated surrounding environment,

polymers display a broad distribution of relaxation times. As *n* increases the breadth of the distribution of relaxation times also increases. Fitzgerald, *et al.* determined that the coupling parameter increased as more SiO_2 was incorporated into the PVAc. This was ascribed to the restriction of the mobility of the PVAc chains due to interactions with the silicate network.

Jensen, *et al.*[4.16] used the concept of cooperativity to model the viscoelastic response of epoxy/E-glass fiber composites. Their characterization technique required the generation of master curves using data acquired from dynamic mechanical analysis. The relative magnitude of the coupling parameter can then be determined by plotting the associated horizontal time-temperature shift factors ($\log a_T$) versus a temperature scale which has been normalized based on a fractional deviation from T_g. Plazek and Ngai[4.14] originally developed the following empirical expression (2) for determining the coupling parameter of bulk polymers using this type of analysis.

$$(1-n)\log a_T = \frac{-C_1(T-T_g)/T_g}{C_2+(T-T_g)/T_g} \qquad (2)$$

This equation is similar in form to the Williams-Landel-Ferry (WLF) equation, except that temperature has been normalized by T_g and the coupling parameter is present. Plazek and Ngai determined that the C_1 and C_2 constants could be universally applied to a wide variety of bulk polymers, having values of 5.49 and 0.141 respectively. The coupling parameter can theoretically vary between 0 and 1, but experimental values of *n* range from 0.45 for polyisobutylene to 0.76 for polyvinylchloride.[4.14] Jensen, *et al.* determined that the coupling parameter of an epoxy matrix increases significantly within this typical range upon the addition of E-glass fibers to the epoxy.

Ngai and Roland[4.17] provided a molecular interpretation of cooperative motion. These researchers proposed that a relatively high level of intermolecular interactions increase the breadth of the distribution of relaxation times in a polymer. If a polymer segment could be isolated as a single unit then at $T = T_g$ this segment would have a unique relaxation time. Under the dense conditions of the solid state the polymer is in close contact with neighboring chains. As thermal energy is raised, a segmental motion begins to occur at T_g and some of the segments cannot relax without involving nonbonded units in the vicinity. The constraining effect due to neighboring chains slows

down the overall relaxation time depending on the volume of the cooperating unity. The coupled segmental relaxations of the polymer chains obviously do not occur at the same time or rate throughout the sample given the heterogeneity of all of the polymer parameters. This leads, phenomenologically, to an increase in the breadth of the distribution of relaxation times. A higher degree of intermolecular coupling and constraints from neighboring segments will increase the amount of cooperative segmental motion required in the transition from the glass to rubber.[4.18] In other words, the segmental motion of neighboring segments is correlated to a greater degree. Polymers with a high amount of cooperativity have viscoelastic properties that exhibit stonger temperature dependence of the time-temperature shift factors in the glass transition region.

The steepness index (S), which is the slope at $T = T_g$ of the cooperativity plot, can be used to calculate the activation energy (E_a) of the glass transition using an Arrhenius relationship through the following set of equations.[4.14, 4.19]

$$S = -T_g\left[\frac{d\log a_T}{dT}\right]_{T_g} = \left[\frac{d\log a_T}{d(T/T_g)}\right]_{T_g} \tag{3}$$

$$\log a_T \propto -\frac{E_a}{2.303RT} \tag{4}$$

$$E_a = 2.303RT_gS \tag{5}$$

In summary of this introduction, cooperativity analysis yields much information on molecular response in complex, multiphase systems. Also, mechanical testing of composites is expensive and time consuming.[4.20] Cooperativity is more quantitative viscoelastic analysis than qualitatively comparing the peak heights or widths of tan δ or loss modulus curves. Cooperativity yields the same conclusions pertaining to the distribution of relaxation times as more complicated fitting procedures. Therefore, this paper will focus in detail about the applicability of cooperativity plots in characterizing the interfacial properties of composite materials. In doing so this will re-emphasize the goal of this work; to investigate a “non-destructive” experimental measure such as cooperativity to qualitatively understand an ultimate property such as strength.

EXPERIMENTAL

Materials and Sample Preparation

The matrix material for the composites was a pultrudable vinyl-ester (see Figure 1) and the composites were all fabricated using the pultrusion processes. Hexcel AS-4 12K unsized carbon fiber (lot # D1317-4C) was sized at Virginia Tech with two different thermoplastic materials: a carboxylic acid poly(hydroxyether)-Phenoxy™ and a poly(vinylpyrrolidone)-K-90 PVP™ (see Figure 2). The Phenoxy™ sizing material (PKHW-35 lot # 217013) was obtained from Phenoxy Associates, Rock Hill, SC. This material was obtained as a 35 weight percent dispersion of approximately 1-micron diameter particles in water. The M_n of the Phenoxy was 19,000 g/mol (GPC) and it had a T_g of 97°C (DSC). The K-90 PVP sizing material (LUVISKOL lot # 20421501) was obtained from BASF. The M_n of this material was 1,250,000 g/mol and it had a T_g of 180°C[4.21]. The K-90 PVP sized fiber had a diameter approximately equivalent to the high-spread Phenoxy. Hexcel AS-4 G′ sized 36K fiber (lot # D1383-5K) was used as the control fiber for these trials and was provided by Strongwell Inc, who also conducted the pultrusion runs. The G′ sizing present on this fiber has been considered the industrial benchmark sizing for the vinyl-ester matrix. Mechanical property data on the two fiber systems utilized in this studied clearly showed that no significant property difference existed between the two fiber lots.

The sized fiber was analyzed for sizing content and consistency using burn-off techniques. No analysis was performed on the commercial G′ sized fiber. Pultrusion was performed at Strongwell using their lab scale pultruder and their standard pultrudable vinyl-ester resin (Derakane 411-35). The die utilized for this study had a cross-section of 0.5″ by 0.075″. The sized fiber spools were loaded into the creel rack and pulled through the resin dip bath. The same resin was utilized for all four pultrusion trials. The composite was then cured in the die. Details regarding the sizing process and the pultrusion of the fiber can be found in an earlier publication.[4.22] The fiber volume fraction of the composite panels produced in these experiments was determined by two methods.[4.23] The first method utilized data collected before the composite part was produced and was termed the theoretical fiber volume fraction. The second method

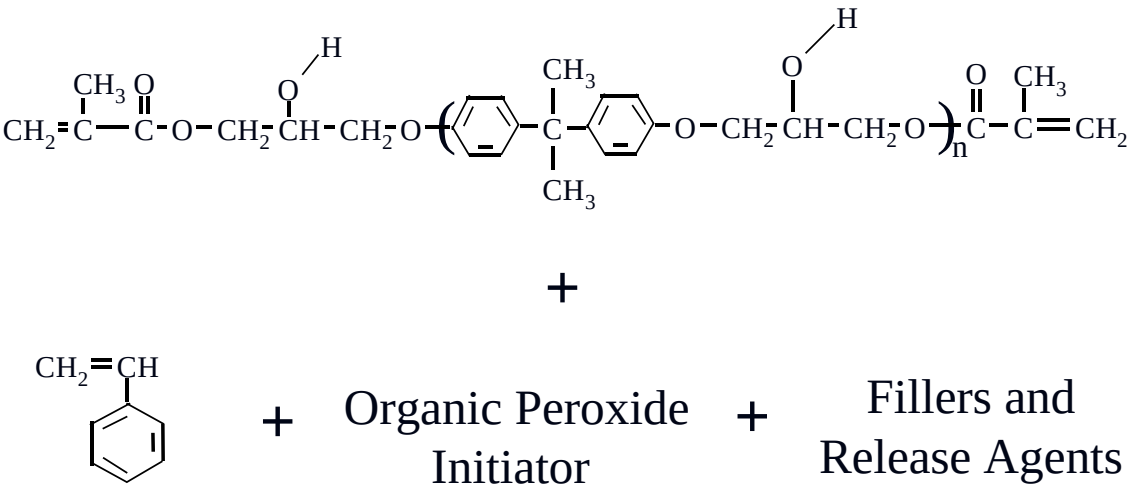

Figure 1: Pultrudable vinyl-ester resin matrix used in graphite composites.

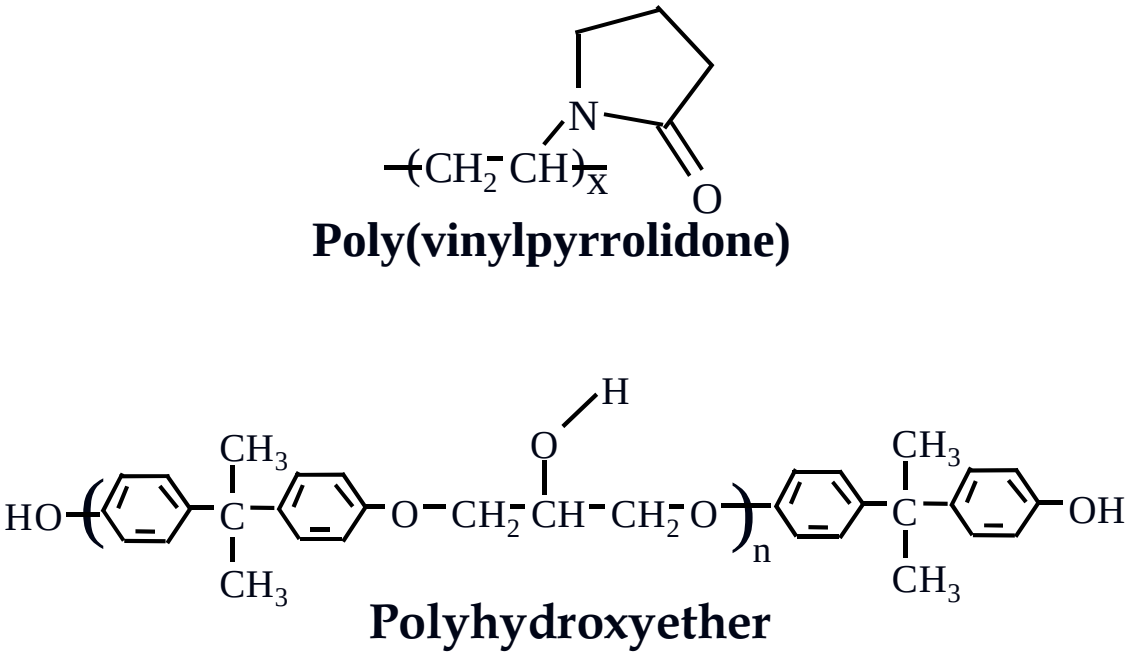

Figure 2: Sizings used to pretreat the graphite fibers.

utilized data collected after the composite part was produced and was termed the experimental fiber volume fraction.

For the first method, the number of tow ends and their respective linear density allowed the determination of the volume of fiber per unit length entering the pultrusion die. The fiber volume fraction could then be computed from the following equation.

$$\nu_f = (n \cdot l_f)/(A_c \cdot \rho_f) \qquad (6)$$

Where, ν_f is the fiber volume fraction, n is the number of tow ends, l_f is the weight per unit length per bundle, A_c is the cross-sectional area of the composite, and ρ_f is the filament density. The cross-sectional area of the composite, A_c, was determined from the die cross-sectional area (neglecting matrix shrinkage) or from the final composite cross-sectional area (including matrix shrinkage). This method neglects the mass of fiber lost in the pre-processing portions of the pultrusion process, which is negligible in most cases. Using equation (6), the theoretical fiber volume fraction of the G" composite was 65.6% and that for the thermoplastic sized composites were 61.1%.

For the second method, the density of the composite was determined and a rule of mixtures was used to determine the fiber volume fraction. A 4g sample of the composite was dried and weighed. The sample was then immersed in isopropyl alcohol and weighed again. The density of the composite was calculated using Archimedes' principle using the following equation

$$\rho_{composite} = W_{air}/(W_{air} - W_{IPA})\,\rho_{IPA} \qquad (7)$$

Where, $\rho_{composite}$ is the density of the composite, ρ_{IPA} is the density of Isopropyl alcohol, W_{air} is the weight of sample in air and W_{IPA} is the weight of sample in isopropyl alcohol. The fiber volume fraction was then calculated using the rule of mixtures

$$\nu = (\rho_{composite} - \rho_{resin})/(\rho_f - \rho_{resin}) \qquad (8)$$

Where, ν is the fiber volume fraction of the composite, $\rho_{composite}$ is the density of the composite calculated from equation (7), ρ_f is the density of the carbon fiber and ρ_{resin} is the density of the cured resin. Equation (8) assumes that the composite has zero void volume. The difficulty in applying equation (8) is that the resin density, ρ_{resin}, is not known exactly. The fiber volume fractions using this method are as follows, 68.0 ± 0.3%, 65.0 ± 0.6%, 61.1 ± 0.6%, and 63.9 ± 0.2% for the G′, LSP, and K-90 PVP sized

composites respectively. Ultrasonic C-scan measurements and cross sectional microscopy was also performed to ensure quality control. Details of the procedure can be found in reference [4.23].

Mechanical Properties Tests

Mechanical property tests included static tension, longitudinal flexure, and short beam shear (SBS). The quasi-static tension tests were performed at room temperature on a servo-hydraulic MTS testing machine. The tests were conducted in load control at a loading rate of approximately 200lbs./sec. The loading cycle was programmed into the Microplrofiler^{TM}. A MTS 448.82 test controller was used to control the machine once the test was started. Strain during the experiments was measured using a 1″ gauge length, MTS Model 632 extensometer. The signal from the extensometer was conditioned using a 2310 Vishay Measurements Group amplifier. The specimens were tabbed using a high-pressure laminated glass-epoxy material. This was done in order to prevent the unidirectional composite samples from crushing in the grips of the machine. The tabs were sand blasted and attached to the specimen using a 3M, DP40 epoxy adhesive. The adhesive was cured in an oven at 50°C for two hours. The grip pressure on the specimen was controlled at 7 MPa. The short beam shear tests were performed in accordance with ASTM D 2344-84, on a screw driven Instron 4104 test frame. The sample length was 11 mm in accordance with the length to thickness ratio for carbon fiber composites. The loading rate of 1.3 mm/min was used.

Dynamic Mechanical Tests

Dynamic mechanical analysis was performed using a Du Pont instruments DMA 983 in flexural bending mode with an amplitude displacement of 0.20 mm peak to peak. The samples were cut with a Behuler Isomet saw using a diamond wafer blade. Typical clamped sample dimensions were 30.0 x 12.8 x 1.9 mm. The primary advantage of using the Du Pont DMA is that the clamp width can be optimized for very stiff composites. The clamp width of 30.0 mm yielded excellent results. The temperature was ramped from 80°C to 220°C in 3°C increments under a nitrogen atmosphere. At each temperature step the viscoelastic response of the composite was measured at frequencies of 0.03, 0.1, 0.3, 1, 3, and 10 Hz. On completion of the measurements at 220°C the

composite specimen was allowed to slow cool to room temperature in the instrument and the measurement procedure was repeated. All of the data used for this paper was taken from the 2nd heat measurements in the DMA. This insures that each sample has the same thermal history. A minimum of four samples were measured for each group of composite specimens.

RESULTS AND DISCUSSION

The dynamic storage modulus curves (E′) obtained at 1 Hz for the composite samples and non-reinforced matrix are illustrated in Figure 3. From this data it is readily apparent that the addition of the graphite fibers significantly increases the modulus of the matrix polymer. The glassy modulus is elevated from approximately $10^{9.5}$ Pa for the matrix to about $10^{10.8}$ Pa for the composites. The composite samples have similar glassy modulus values. The rubbery modulus is also much higher in the composites than in the non-reinforced matrix. The G′ sizing yielded the highest rubbery modulus, while the Phenoxy and PVP sized fiber samples have similar values of rubbery modulus. The increased value of rubbery modulus for the G′ sized fiber samples could be due to a slightly higher volume fraction of fibers. The glass-to-rubber transition regions of the composite samples are also much broader than in the non-reinforced matrix.

A closer examination of the glass-to-rubber transition of the composites and the non-reinforced matrix can be seen in the normalized tan δ curves (1 Hz) shown in Figure 4. The matrix has the highest T_g (138°C), as defined by the peak maximum of the α-transition. This could probably be due to the absence of processing aids which are typically added in the pultrusion process, which could act as plasticizers in depressing the glass transition temperature. The T_g's of the composite samples range from 116°C for the G′ sized fiber sample to 122°C and 125°C for the Phenoxy and PVP sized fiber samples respectively. The α-transition of the PVP and Phenoxy sized composite samples was taken as the low temperature shoulder that is present in the tan δ curves. Both the PVP and Phenoxy sized fiber composites exhibit a distinct second transition peak above 150°C. The shoulders on the Phenoxy and PVP curves both occur near the same temperature as the α-transition peak of the G′ curve. The higher temperature transitions evident in the Phenoxy and PVP sized fiber composites could be the glass transitions of

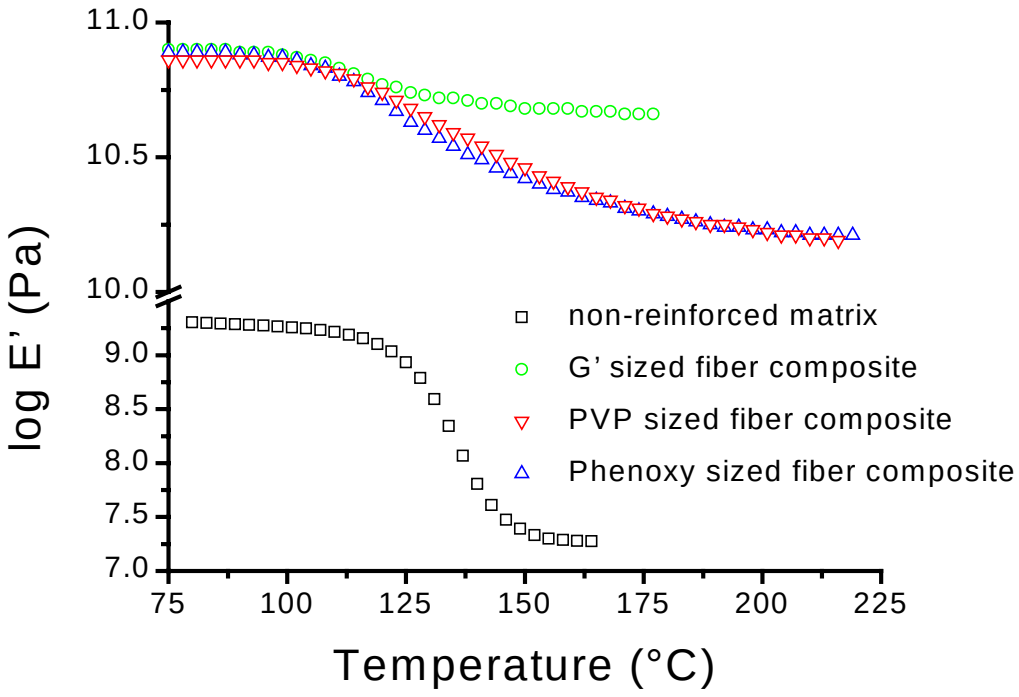

Figure 3: Storage modulus curves for graphite composite samples as well as non-reinforced matrix versus temperature obtained from DMA (1 Hz).

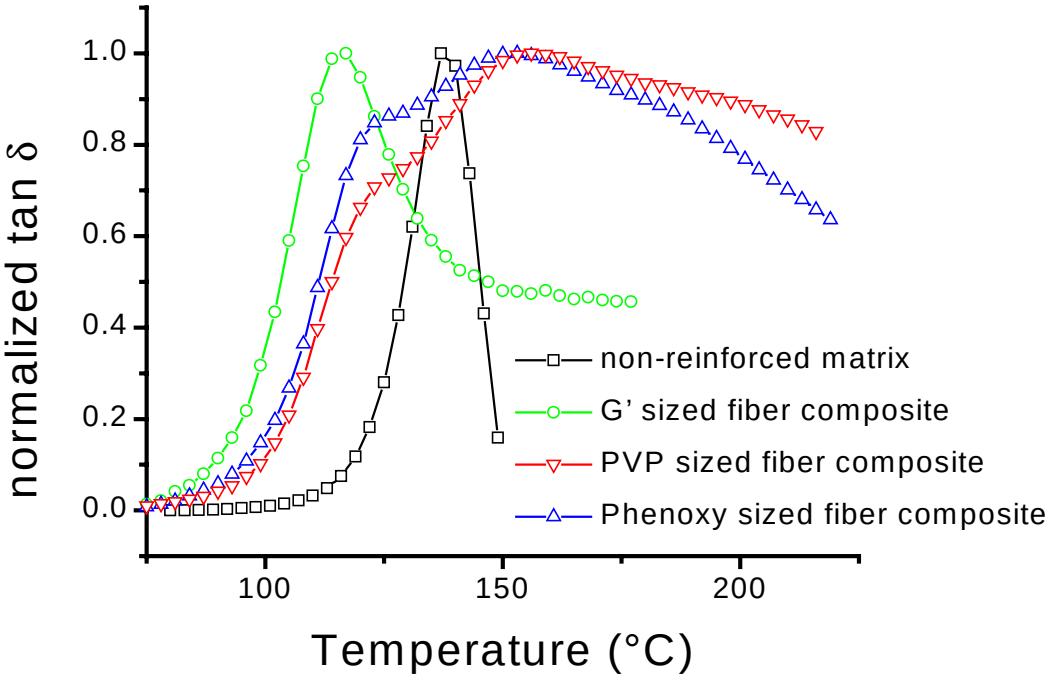

Figure 4: Normalized tan δ curves obtained from DMA measurements (1 Hz).

the sizings themselves, or a highly restricted interphase region near the fiber surface. The higher temperature transitions evident in the tan δ curves were very consistent and reproducible. Thomason[4.10] published results which indicate that a high temperature peak in the loss modulus or tan δ curves of a fiber-reinforced composite could be an artifact of the DMA due to thermal lag in the sample. However, in our case the measurement technique used for these experiments, the step-isothermal mode, precludes such a lag. Specifically, the DMA increases temperature in 3°C increments, equilibrates at the designated temperature, and then sweeps the assigned frequencies. The low frequency measurement (0.03 Hz) is responsible for making this procedure much slower than a more common constant heating rate experiment. Total measurements (from 80°C to 220°C) were typically completed overnight with 25 - 30 minutes required at each individual temperature step. Due to the lengthy step times that the composites experienced in the DMA, confidence can be placed in the judgement that the additional high temperature tan δ peaks in the Phenoxy and PVP samples are not artifacts.

The composite samples also have tan δ curves that are much broader than the non-reinforced matrix. This increased peak broadness and absence of the second transition in the storage modulus curves is consistent with the findings of Lewis and Nielsen.[4.5] The transition temperatures obtained from the tan δ curves are summarized in Table1.

Table 1: Summary of transition temperatures in non-reinforced matrix and fiber composite samples.

sample	**T_g (α-transition)**	**$T_{second\ transition}$**
non-reinforced matrix	138°C	not present
G' sized fiber composite	116°C	not present
PVP sized fiber composite	125°C	159°C
Phenoxy sized fiber composite	122°C	152°C

Figure 5 depicts the normalized dynamic loss modulus curves (E″) curves for the various samples. The same trends are evident in the loss modulus as were seen in the tan δ data previously discussed.

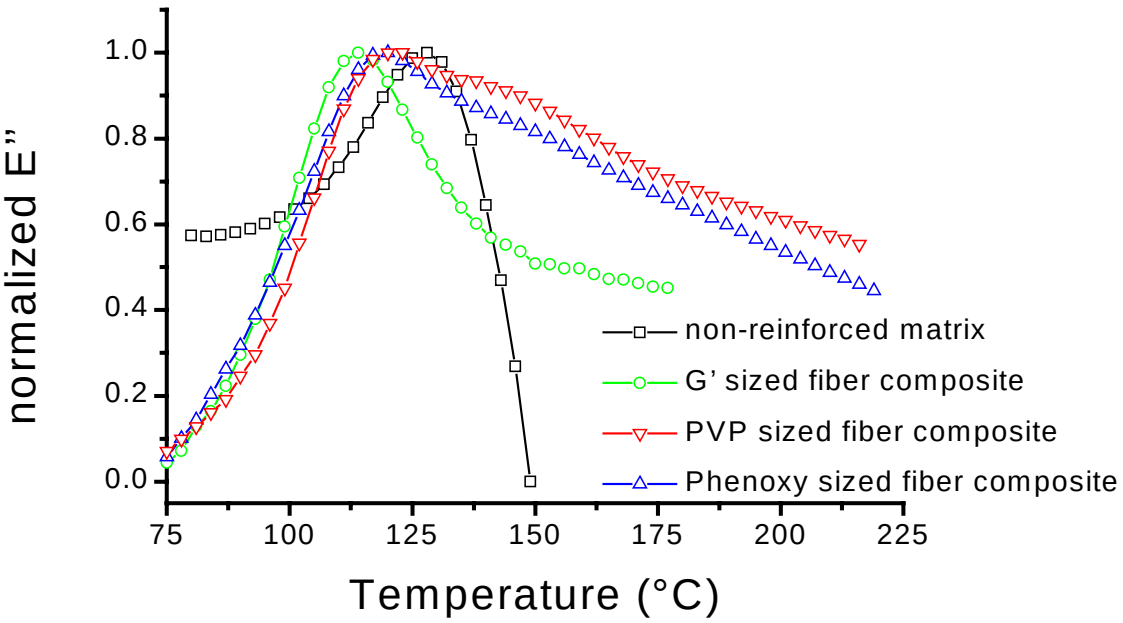

Figure 5: Normalized loss modulus curves obtained from DMA measurements (1 Hz).

Master Curves

The time-temperature superposition (tTSP) procedure was used to construct master curves of the storage modulus in the frequency domain for each of the samples studied. The glass transition temperatures, measured at 1 Hz from the tan δ curves, were used as the reference isotherms. Master curves were successfully created from the storage modulus data without any vertical shifting. However, this was not the case for the loss modulus data. Vertical shifting of the loss modulus curves is required for the composite samples. This could be due to multiple relaxation mechanisms occurring simultaneously within the matrix, sizing, and/or interphase region. No trends were apparent with respect to the vertical shifting of the loss modulus curves. Sullivan, *et al.*.[4.20] also observed that vertical shifting was required for tTSP in vinyl ester/E-glass composites. These researchers also found no clear trends with regard to the vertical shift factors. The loss modulus data may be overly sensitive for the application tTSP, but the storage modulus data was acceptable.

Figure 6 shows the normalized storage modulus curves for the composite and non-reinforced matrix samples. The composite sample master curves were slightly noisier, but highly reproducible. The fiber reinforcement extents the glass-to-rubber transition zone to much lower frequencies, or longer times, than the non-reinforced matrix. The Phenoxy sample extends to the lowest frequencies, followed by the PVP and G′ samples respectively.

Cooperativity

Horizontal shift factor values were obtained from the generation of the master curves. Cooperativity plots were then produced following the analysis of Plazek and Ngai.[4.17] The cooperativity plots are illustrated in Figure 7. The cooperativity of the composite samples clearly varies depending on the sizing that was used to pretreat the fibers. Again, these plots were very reproducible. At least four samples were run for each sizing and the standard deviation is negligible compared to the absolute values. The log a_T values for the composite samples are found to have greater temperature sensitivity than the non-reinforced matrix, resulting in the high slopes in Figure 7. The Phenoxy sized fiber composite shows the greatest temperature dependence, followed closely by the PVP sized sample. The G′ sample has an intermediate steepness between the matrix and

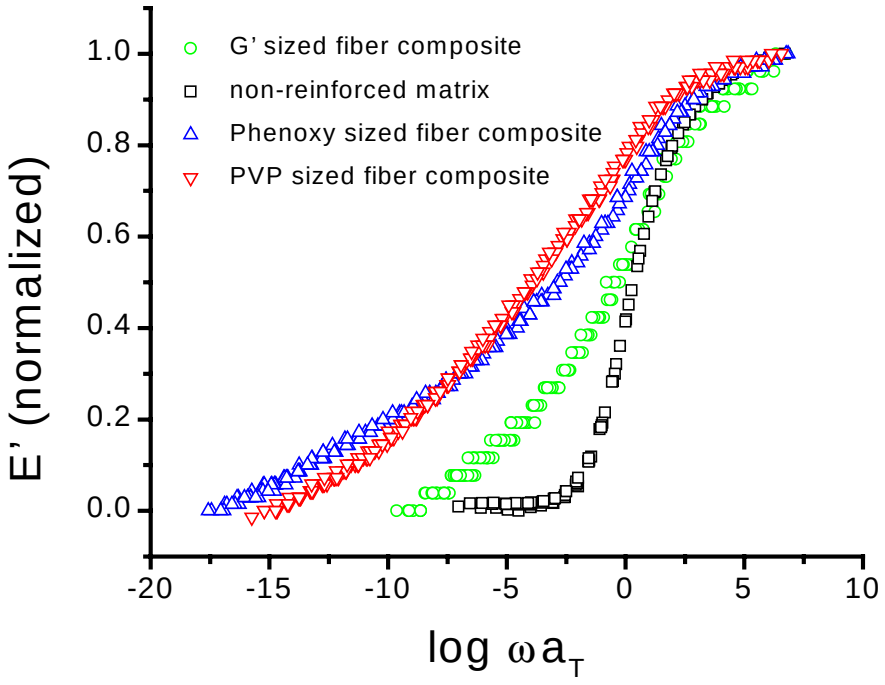

Figure 6: Normalized storage modulus master curves.

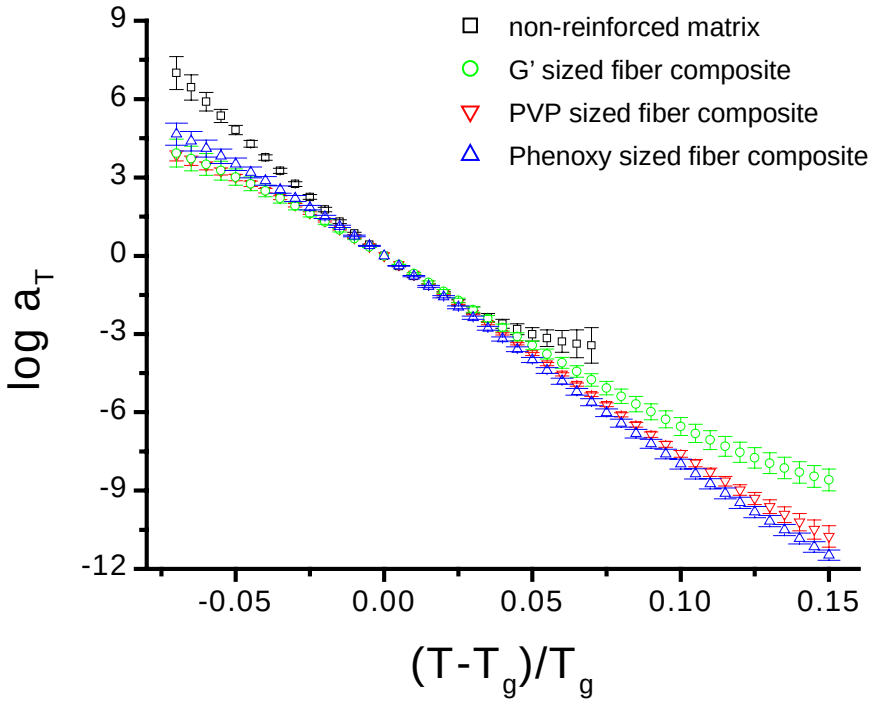

Figure 7: Cooperativity plots at temperatures above and below T_g.

the PVP sample. All of the composite samples exhibit similar behavior in the glassy state, which differs from the matrix sample. This similarity in viscoelastic behavior of the samples at the glass transition is also observed in the calculated values of S and E_a at $T = T_g$ (Table 2). The trends in cooperativity are apparent. The non-reinforced matrix has the highest activation energy at $T = T_g$.

Table 2: Coupling parameters and steepness indexes.

Sample	***n***	**S**	**E_a (KJ/mol)**
non-reinforced matrix	0.510 (± 0.014)	82.2 (± 5.3)	647 (± 42)
G' sized fiber composite	0.649 (± 0.219)	66.0 (± 3.9)	492 (± 28)
PVP sized fiber composite	0.702 (± 0.624)	69.8 (± 2.9)	532 (± 22)
Phenoxy sized fiber composite	0.718 (± 0.705)	75.6 (± 3.3)	574 (± 27)

As can be seen from Equation 5, the activation energy is determined from the slope of the cooperativity plot at $T = T_g$. The non-reinforced matrix has the steepest slope in the glassy state, which is closer to the equilibrium behavior predicted by Equation 2. The non-reinforced matrix would not be restricted in mobility by the glass fibers and should have less free volume upon cooling, at the same rate, leading to an increase in E_a. Sullivan, *et al*.[4.20] determined that the viscoelastic relaxation times of E-glass composites seem to be universal in the glassy and short time regions near T_g.

The cooperativity plots of the composites can also be extended to much higher temperatures, above T_g, than the non-reinforced matrix. As can be seen from the master curves, the rubbery modulus of the composites does not level off to a plateau value. This is why tTSP of the E′ data can be extended to temperatures greater than T_g in the composite samples. The fiber reinforcement must have a key influence on the relaxation of the matrix phase at temperatures much greater than T_g.

Figure 8 shows an expanded view of the cooperativity plots at $T > T_g$ for all of the samples. The curves have also been best fit to equation 2 using a non-linear regression. The analysis of Plazek and Ngai provides a reasonable description of the viscoelastic behavior of the non-reinforced matrix using the literature values for the

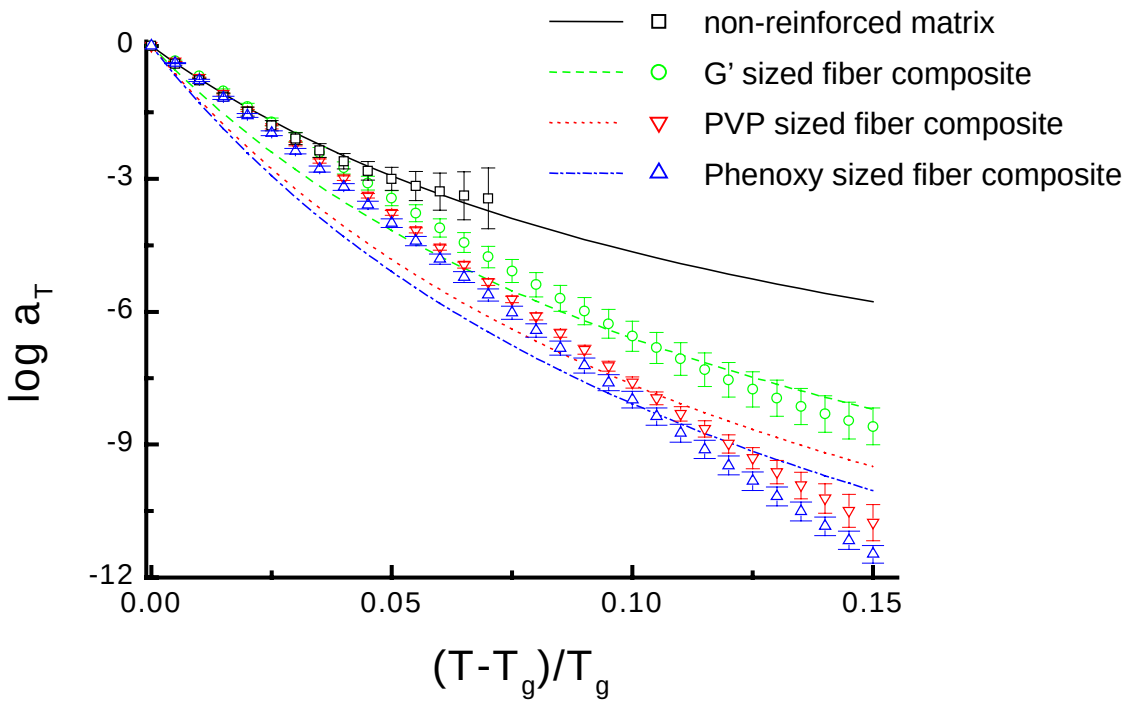

Figure 8: Cooperativity plots at $T > T_g$ with best fit approximations of *n* using equation 2.

constants C_1 and C_2. Equation 2 does not accurately fit the cooperativity data of the composite materials. Equation 2 predicts a curve that is concave up and that gradually levels off at $T >> T_g$. While the log a_T values for the non-reinforced matrix begin to plateau at temperatures approximately 30°C greater than T_g, where $(T-T_g)/T_g \approx 0.05$, the log a_T values for the fiber reinforced composites continue to steadily increase in value. Therefore, the cooperativity plots of the composites are closer to linear in shape and cannot be reasonably fit to equation (2). At temperatures close to T_g all of the samples display nearly identical cooperativity. The curves begin to separate near T_g + 20°C, where $(T-T_g)/T_g \approx 0.04$, and can be distinguished at this point. The effect of the fiber sizing becomes more pronounced at $T > T_g$ + 30°C. This indicates that the viscoelastic behavior of the polymeric component of a composite material is more complicated and is altered by the presence of the fibers. The failure of equation (2) to fit to the composite data could be indicative of multiple over-lapping relaxation mechanisms. If the fiber-matrix interphase, created through the interdiffusion of the individual species during fabrication, is restricted in mobility then the relaxation of this region would occur at a higher temperature than the non-reinforced bulk matrix phase. The calculated *n* values have also been summarized in Table 2.

Mechanical Properties

Figure 9 shows the quasi-static tensile strength for the individual composites. As it can be seen, the G′ sizing did not perform as well as the Phenoxy and PVP sizings. Further, a relationship seems to connect the mechanical data, one which tends to be corroborated by the viscoelastic data shown in Figure 8. It appears to that the composite with the greatest cooperativity tends to be the strongest in tension. The tensile modulus is depicted in Figure 10. Figure 11 shows the apparent shear strength obtained from short beam shear test data. An identical trend seems to exist as compared to the tensile strength data. The trends in the data seem to indicate that the process of fracture that tends to dominate in measurement of strength in a unidirectional composite can be influenced by the type of sizing polymer that is applied on the fiber. The interphase that develops via interdiffusion of the sizing polymer and the matrix resin indicates differences in terms of the composite's viscoelastic response, especially with respect to the packing features as it cools to form the glass. This is clearly depicted through the

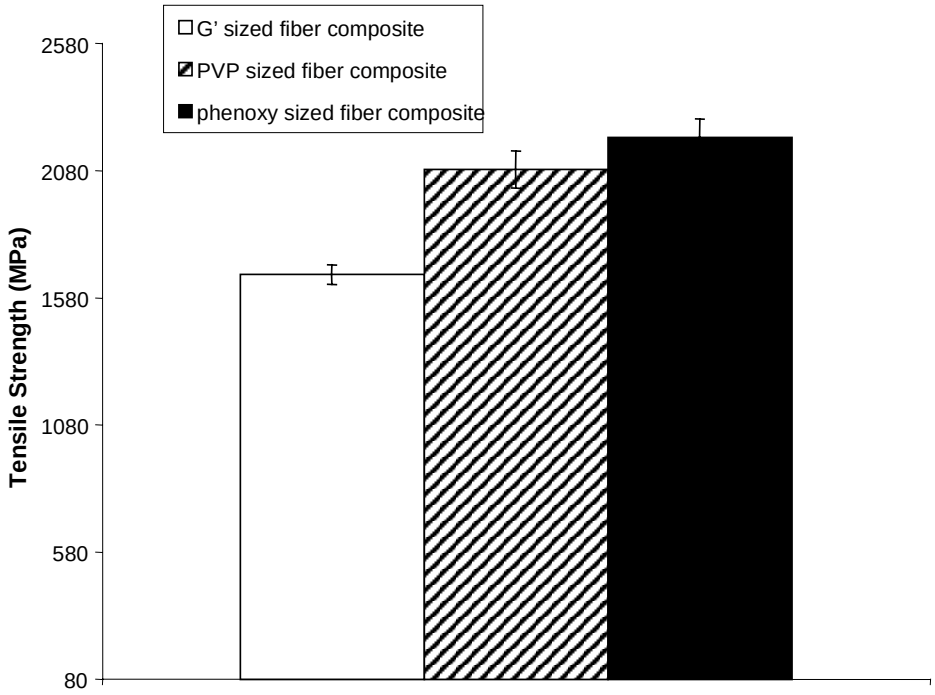

Figure 9: Tensile strength of unidirectional carbon fiber/ vinyl ester composites with different sizings.

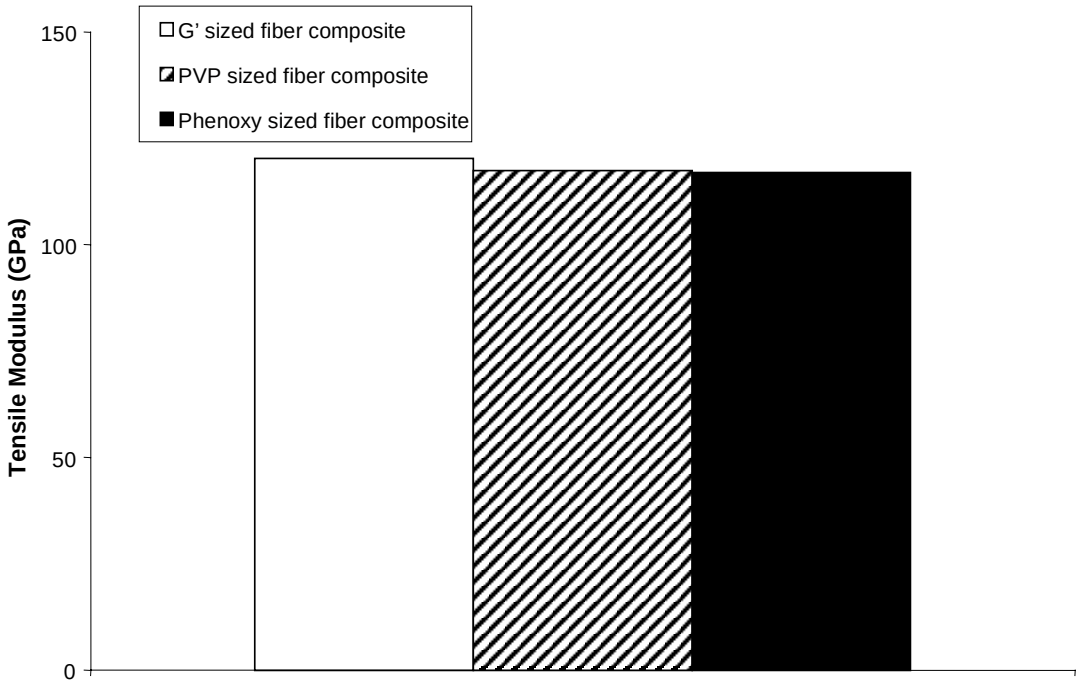

Figure 10: Tensile modulus of unidirectional carbon fiber/ vinyl ester composites with different sizings.

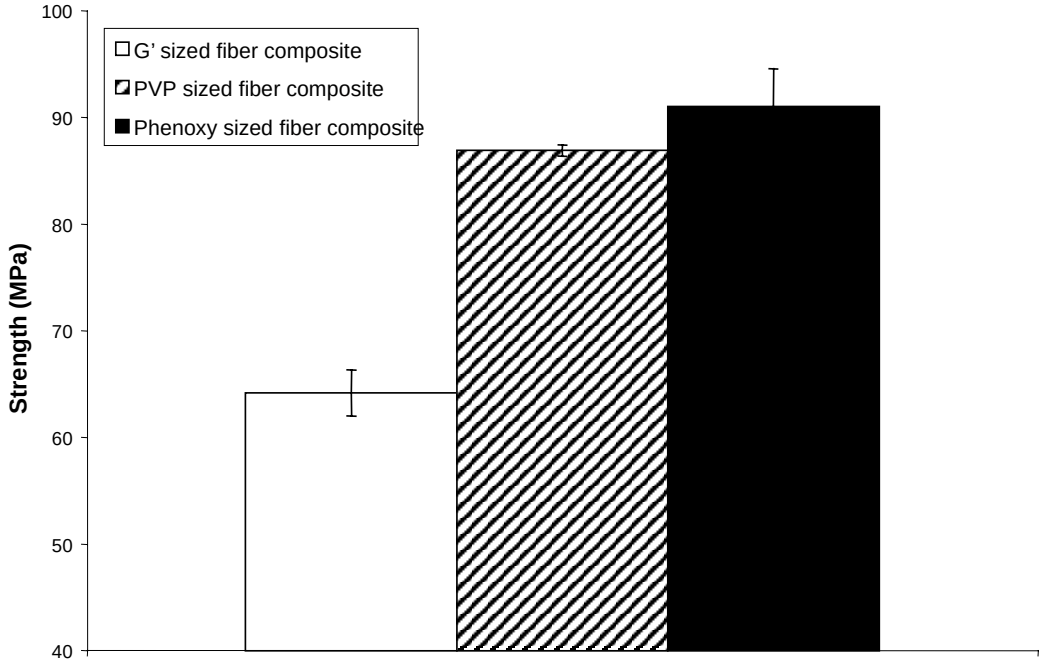

Figure 11: Apparent shear strength of unidirectional carbon fiber/ vinyl ester composites with different sizings.

cooperativity results presented above. In this study, since carbon fiber was the only reinforcement used, the high temperature transition is possibly a reflection of the existence of an interphase region. Speculating, the resin at the interphase region could be highly constrained. In work done by Shan, *et al*.[4.24] it was observed that the packing features dramatically influenced the fracture toughness of the polymer. Their study looked at the effect of network architecture on the viscoelastic behavior of vinyl ester resin. The effect of changing the molecular weight between crosslinks was clearly seen to influence the cooperativity or fragility analysis. Further, a strong correlation seemed to exist between the fracture toughness of the polymer and a normalized quantity that involved the cooperative domain size and the molecular weight between crosslinks. From this, it can be suggested that the increase in tensile strength of the composites was due to the increased fracture toughness at the interphase, an inference that was confirmed from the viscoelastic (cooperativity) studies. A similar observation has been made by Rosen[4.25] while trying to identify the mechanism of tensile failure in unidirectional composites. He describes the importance of having a tough matrix especially when the bonding to the fiber is good in order to prevent the propagation of the initial crack, across the composite causing premature failure. In addition to the above discussed mechanical properties, the interphase has also been reported to have a dramatic influence on the fatigue response (durability) of composites.[4.22]

CONCLUSIONS

In the present paper, the thermal dependence of intermolecular cooperativity, has been explored for carbon fiber reinforced, unidirectional composites with different sizings. It was observed that the shape of the curve changes considerably moving from the neat resin to the composite. This is primarily because of the fibers that pack the polymer, which act as a continuous filler phase. These fillers tend to retard the relaxation process considerably by adding additional constraints to the bulk matrix. Mechanical test data on these pultruded composites indicate a strong correlation between tensile strength and relaxation behavior. This was found to agree well with the coupling idea which states that the relaxation behavior of polymers is not only affected by intramolecular coupling restrictions but also intermolecular interactions. London dispersion forces,

hydrogen bonding, polar interactions, network formation, fillers etc. can all be included in this category of intermolecular restrictions. Materials that are more sterically restricted tend to relax cooperatively rather than individually giving rise to higher coupling parameters. The Phenoxy sizing, which had the highest coupling (cooperativity) parameter, exhibited the highest strength. The order for both tensile strength and coupling parameter are as follows, vinyl ester matrix < G′ < PVP < Phenoxy. This connection between the viscoelastic behavior and both the fracture toughness and tensile strength of the composite was speculated to be due to similar origins. It is well known that strength is a fracture controlled process and so such a correlation may be likely. In the authors' view, the ability to draw qualitative connections between molecular behavior and specimen level macroscopic strength are invaluable especially considering the range of material structure that is covered and the possibility of using such a technique as a screening tool.